Computation Rate Maximization for Intelligent Reflecting Surface Enhanced Wireless Powered Mobile Edge Computing Networks

Sun Mao ⓘ, Ning Zhang ⓘ, *Senior Member, IEEE*, Lei Liu ⓘ, *Member, IEEE*, Jinsong Wu ⓘ, *Senior Member, IEEE*, Mianxiong Dong ⓘ, *Member, IEEE*, Kaoru Ota ⓘ, *Member, IEEE*, Tang Liu, and Die Wu

Abstract—The combination of wireless energy transfer (WET) and mobile edge computing (MEC) has been proposed to satisfy the energy supply and computation requirements of resource-constrained Internet of Things (IoT) devices. However, the energy transfer efficiency and task offloading rate cannot be guaranteed when wireless links between the hybrid access point (HAP) and IoT devices are hostile. To address this problem, this paper aims at utilizing the intelligent reflecting surfaces (IRS) technique to improve the efficiency of WET and task offloading. In particular, we investigate the total computation bits maximization problem for IRS-enhanced wireless powered MEC networks, by jointly optimizing the downlink/uplink phase beamforming of IRS, transmission power and time slot assignment used for WET and task offloading, and local computing frequencies of IoT devices. Furthermore, an iterative algorithm is presented to solve the non-convex non-linear optimization problem, while the optimal transmission power and time allocation, uplink phase beamforming matrixes and local computing frequencies are derived in closed-form expressions. Finally, extensive simulation results validate that our proposed IRS-enhanced wireless powered MEC strategy can achieve higher total computation rate as compared to existing baseline schemes.

I. INTRODUCTION

A. Background

WITH the rapid development of Internet of Things (IoT), a variety of emerging intelligent services (e.g., smart home, autonomous driving, telemedicine) have imposed great challenges for resource-constrained IoT devices with restricted energy supply and poor computing capacity [1]–[5]. In order to address this bottleneck, wireless powered MEC is considered as a thriving technique to enable sustainable energy supply and low-delay computing services for massive IoT devices [6]–[10]. In wireless powered MEC networks, an hybrid access point (HAP) equipped with an edge server is deployed to provide wireless charging and task offloading services for IoT devices. However, the performance of wireless powered MEC networks cannot be guaranteed when wireless channels between the HAP and IoT devices are blocked occasionally by some static or moving objects.

Currently, intelligent reflecting surface (IRS) has been considered as an innovative technique to reconfigure the wireless communication environment [11]–[14]. In general, the IRS is an integrated panel comprised by a controller circuit and a massive number of low-cost reflection units, which can intelligently adapt the amplitudes and phases of incident signals for achieving fine-grained reflect beamforming [15], [16]. In wireless powered MEC networks, IRSs can be properly deployed and controlled to improve the energy transfer efficiency and task offloading rate. Besides, the total computation rate is a key performance indicator to reveal the computing capability of MEC networks. Therefore, this paper concentrates on developing a novel framework for realizing IRS-enhanced wireless powered MEC networks to maximize the total computation rate.

B. Related Works

The existing research works can be summarized from three perspectives, namely resource management for wireless powered MEC networks, IRS-assisted wireless energy transfer, and IRS-assisted mobile edge computing.

Sun Mao is with the College of Computer Science, Sichuan Normal University, Chengdu 610101, China (e-mail: sunmao@std.uestc.edu.cn).

Ning Zhang is with the Department of Electrical and Computer Engineering, University of Windsor, Windsor, ON N9B 3P4, Canada (e-mail: ning.zhang@ieee.org).

Lei Liu is with the State Key Laboratory of Integrated Service Networks, Xidian University, Xi'an 710071, China (e-mail: tianjiaoliulei@163.com).

Jinsong Wu is with the Department of Electrical Engineering, Universidad de Chile, Santiago 8370451, Chile (e-mail: wujs@ieee.org).

Mianxiong Dong is with the Department of Sciences and Informatics, Muroran Institute of Technology, Muroran 050-8585, Japan (e-mail: mx.dong@csse.muroran-it.ac.jp).

Kaoru Ota is with the Department of Information and Electronic Engineering, Muroran Institute of Technology, Muroran 050-8585, Japan (e-mail: ota@csse.muroran-it.ac.jp).

Tang Liu and Die Wu are with the College of Computer Science, Sichuan Normal University, Chengdu 610101, China (e-mail: liutang@sicnu.edu.cn; dwu.cse@gmail.com).

Digital Object Identifier 10.1109/TVT.2021.3105270

1) Resource Management for Wireless Powered MEC Networks: Wireless powered mobile edge computing has attracted extensive attentions from academia, since it can satisfy the sustainable low-delay computing requirements of IoT devices. In order to exert all the advantages of wireless powered MEC networks, it is essential to design joint energy, communication and computation resource scheduling strategy. In [17], You *et al.* first proposed a wireless powered MEC framework, and they further investigated the computing probability maximization problem under the energy casuality and computing delay constraints. Under this framework, the authors in [18] and [19] studied the power consumption minimization and computation rate maximization problems, respectively. In addition, our work in [20] revealed the tradeoff relationship between network energy efficiency and task processing delay for wireless powered MEC networks. However, the limited edge computing capability may fail to meet the computation requirements from massive IoTs. Therefore, these works in [21], [22] proposed the user communication/computing cooperation strategy for enhancing the performance of wireless powered edge computing. Furthermore, Zhou *et al.* in [23] and [24] utilized the mobility of unmanned aerial vehicles base station and non-orthogonal multiple access technique to improve the energy transfer efficiency and task offloading rate.

2) IRS-Assisted Wireless Energy Transfer: IRS has been extensively utilized to improve the efficiency of radio-frequency based wireless energy transfer. In [25], Wu *et al.* first investigated the sum harvested power maximization problem for a single IRS-assisted WET system. This research work was extended to the scenario with multiple IRSs in [26], and they developed a penalty function-based method to address the total power consumption minimization problem. Pan *et al.* in [27] considered to exploit the multiple antennas technique to improve the energy/information transfer efficiency for IRS-assisted WET systems. Furthermore, Lyu *et al.* in [28] studied an IRS-empowered wireless powered communication network (WPCN), in which the IRS can exploit the harvested downlink energy to assist energy/information transfer between the HAP and mobile terminals. In [29], Bi *et al.* exploited the IRS to enhance the energy efficiency for a WPCN with user cooperation. To achieve the convenient and low-cost energy supply for IRSs, the authors in [30], [31] proposed wireless powered IRS framework, in which the reflection element of IRS can be adjusted to harvest the radio-frequency energy for satisfying its energy requirements.

3) IRS-Enhanced Mobile Edge Computing: The potential of MEC cannot be fully released when the communication links for task offloading are hostile. Therefore, some works introduced IRS into MEC systems to improve the task offloading rate. The authors of [32], [33] investigated the latency minimization problem for infrastructure-based MEC networks. In order to exploit the spare computing resources of IoT devices, our work in [34] designed the delay-oriented resource allocation algorithm for IRS-assisted device-to-device (D2D) cooperative computing systems. In addition to the computing delay, the total computation bits is another key performance indicator to evaluate the total computing capability for MEC networks. Therefore, Chu

et al. in [35] focused on maximizing the total computation rate for a multi-user IRS-assisted MEC network. Considering the high computational complexity of conventional optimization methods, Hu *et al.* in [36] proposed the deep learning-based architecture to achieve online task offloading and resource scheduling for IRS-assisted multi-user MEC networks. In [37], Liu *et al.* studied the earning maximization problem under the computation bits constraints of mobile devices. In [38], Bai *et al.* put forward an IRS-assisted wireless powered MEC framework, and they further proposed a joint energy, communication and computation resource scheduling approach for minimizing the system total power consumption.

C. Novel Contributions

Although the resource scheduling problems have been extensively investigated in wireless powered MEC networks [17]-[24], few works considered to utilize the IRS to improve the efficiency of WET and task offloading. Moreover, the power consumption of IRS was generally ignored in existing IRS-enhanced wireless networks. In practice, the power consumption of IRS increases linearly with the number of reflection units and a massive number of reflection units are usually installed on an IRS to improve the reflecting beamforming gain [30], [31].

Motivated by these observations, this paper considers a novel IRS-assisted wireless powered MEC network, and we mainly investigate the resource allocation strategy to coordinate the wireless charging for the IRS and IoT devices, and the task offloading of IoT devices. The main contributions of this work are summarized as follows.

- We present a novel IRS-enhanced wireless powered MEC network framework that exploits the IRS technique to improve the efficiency of energy transfer and computation offloading. In this framework, the IRS first receives the downlink energy signal from the HAP, and then utilizes the harvested energy to assist both the downlink energy transfer and the uplink task offloading between the HAP and IoT devices.
- We propose a total computation bits maximization problem under the energy casuality constraints of IRS and IoT devices, with the joint optimization of the downlink/uplink phase beamfroming of IRS, transmission power and time slot allocation for WET and computation offloading, and local computing frequencies of IoT devices.
- We design an alternative optimization method to solve the proposed non-convex non-linear computation bits maximization problem. Specifically, we further derive the closed-form solutions for uplink phase beamforming of IRS, time slot allocation, transmit power and local computing frequencies of IoT devices, while the variable substitute and semi-definite relaxation technique are used to solve the downlink phase beamforming optimization subproblem.

The remainder of this work is outlined as follows. The system model and frame structure are presented in Section II. The total computation bits maximization problem is investigated in
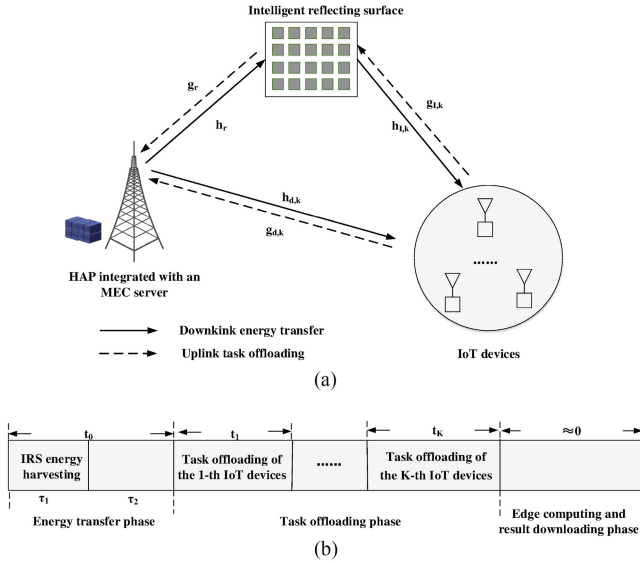
Fig. 1.   IRS-assisted wireless powered MEC networks.

Section III. The simulation results are provided in Section IV. Section V concludes this paper.

Notations: $\mathbf{a}^T$, $\mathbf{a}^H$, diag($\mathbf{a}$), and arg($\mathbf{a}$) are the transpose, Hermitian transpose, diagonalization, and phase of the vector $\mathbf{a}$, respectively. For a matrix $\mathbf{A}$, Tr($\mathbf{A}$) stands for its trace, whereas $[\mathbf{A}]_{mn}$ represents its element in the m-th row and n-th column.

II. SYSTEM MODEL

As illustrated in Fig. 1(a), we consider an IRS-enhanced wireless powered MEC systems which comprises a HAP equipped with an edge server, K energy-constrained IoT devices indexed by $\mathcal{K} \in \{1, 2, \ldots, K\}$, and an IRS with M reflecting units denoted by $\mathcal{M} = \{1, 2, \ldots, M\}$. Similar to [17]-[24], we suppose that the IoT devices and IRS have no any embedded energy supply, and they have to collect downlink energy transmitted by the HAP. Each IoT device can utilize the harvested energy for executing its computing tasks through local computing or task offloading. Moreover, the IRS is properly deployed to improve the efficiency of energy transfer and computation offloading, by adjusting the phases of downlink/downlink incidents signals for achieving fine-grained reflect beamforming.

The downlink channel coefficients from the HAP to the k-th IoT device, from the HAP to the IRS, and from the IRS to the k-th IoT devices will be expressed as $h_{d,k}$, $\mathbf{h}_r \in \mathbb{C}^{M \times 1}$ and $\mathbf{h}_{I,k}^H \in \mathbb{C}^{1 \times M}$, respectively. Moreover, the counterpart uplink channels are represented by $g_{d,k}$, $\mathbf{g}_r^H \in \mathbb{C}^{1 \times M}$ and $\mathbf{g}_{I,k} \in \mathbb{C}^{M \times 1}$, respectively. All the channels follow block fading, and remain constant during the current time block but may change at the boundaries of time blocks [23], [24]. In addition, we suppose that the perfect channel state information can be obtained by the HAP by using the advanced channel estimation scheme.

As depicted in Fig. 1(b), the entire time block with duration T seconds mainly includes three phases, i.e., the downlink energy transfer phase, the uplink task offloading phase, and the edge computing and result downloading phase.

A. Energy Transfer Phase

At the beginning of the time block, the HAP first conducts the downlink wireless charging for the IRS and IoT devices. In particular, the energy transfer phase with duration t_0 will be further partitioned into two sub-slots, with durations of τ_1 and τ_2, respectively, which satisfies $\tau_1 + \tau_2 = t_0$.

In the first sub-slot τ_1, the IRS operates in energy harvesting mode for collecting the radio-frequency energy from the HAP. We define $\eta \in (0, 1]$ and P_0 as the linear energy conversion efficiency and downlink transmission power of the HAP, respectively. Therefore, the energy harvested by the IRS during τ_1 can be calculated as

$$E_I = \eta \tau_1 P_0 \|\mathbf{h}_r\|^2, \tag{1}$$

Note that the noise power is generally much smaller than the power of downlink energy signals [39]–[41], and thus is neglected in (1).

In the second sub-slot τ_2, the IRS will exploit part of its harvested energy to assist the downlink energy transfer from the HAP to IoT devices. The reflection matrix of the IRS is given by $\Gamma_d = \text{diag}\{e^{j\theta_{d,1}}, \ldots, e^{j\theta_{d,M}}\}$, where j denotes the imaginary unit, and $\theta_{d,m} \in [0, 2\pi]$ stands for the phase shift of the m-th passive unit. Besides, the IRS controller is able to control the phase shifts of reflection units, according to the resource scheduling results transmitted by the HAP. Therefore, the harvested downlink energy of the k-th IoT device will be

$$E_k = E_{k,1} + E_{k,2}, \tag{2}$$

where $E_{k,1} = \eta \tau_1 P_0 |h_{d,k}|^2$ and $E_{k,2} = \eta \tau_2 P_0 |\mathbf{h}_{I,k}^H \Gamma_d \mathbf{h}_r + h_{d,k}|^2$ represent the harvested energy of the k-th IoT device at the first and second sub-slots, respectively.

B. Task Offloading Phase

In the second phase, the IoT devices can exploit the harvested energy to process their tasks via local computing and computation offloading.

1) Local Computing: Each IoT device can utilize the remaining time block with duration $T - t_0$ to perform local computing. C_k denotes the tasks' computational complexity at the k-th IoT device. Therefore, the size of locally computed bits and the computing energy consumption at the k-th IoT device are given by

$$D_{k,loc} = \frac{f_k(T - t_0)}{C_k}, \tag{3a}$$

$$E_{k,loc} = \kappa(T - t_0)f_k^3, \tag{3b}$$

respectively. f_k represents the computing speed at the k-th IoT device. κ stands for the effective capacitance coefficient, which depends on the hardware architecture [42], [43].

2) Task Offloading: Except for local computing, the IoT devices also can transmit their computing tasks to the HAP in a time-division manner. Defining P_k and t_k as the transmission

power and offloading duration of the k-th IoT device, respectively. Thus, the offloading bits by the k-th IoT device will be

$$D_{k,off} = Bt_k \log_2 \left(1 + \frac{P_k|\mathbf{g}_r^H \Gamma_{u,k} \mathbf{g}_{I,k} + g_{d,k}|^2}{\delta^2} \right), \quad (4)$$

where B denotes the total network bandwidth, $\Gamma_{u,k} = \mathrm{diag}\{\beta_{U.K.1}e^{j\theta_{U.K.1}}, \ldots, \beta_{U.K.M}e^{j\theta_{U.K.M}}\}$ is the uplink reflecting coefficient matrix of the IRS during the k-th offloding time slot t_k, where $\theta_{U.K.m}$ is the uplink reflection phase shift of the m-th passive unit, and δ^2 represents the noise power.

3) Edge Computing and Result Downloading: After the phase of task offloading, the edge server will execute the received computation tasks from IoT devices and then return the corresponding results to IoT devices. Since the edge server has powerful computing capability compared with IoT devices and the size of computation results is relatively small, thus this work ignores the process of edge computing and result downloading [44]–[46].

According to above descriptions, the total accomplished computation task of the k-th IoT device will be

$$\begin{aligned} D_k &= D_{k,loc} + D_{k,off} \\ &= \frac{f_k(T - t_0)}{C_k} + Bt_k \log_2 \left(1 + \frac{P_k|\mathbf{g}_r^H \Gamma_{u,k} \mathbf{g}_{I,k} + g_{d,k}|^2}{\delta^2} \right) \end{aligned}$$
$$(5)$$

C. Energy Consumption Model

The total energy consumption at the k-th IoT device consists of both the communication and computation energy consumption, which cannot exceed its harvested energy, i.e.,

$$E_{c,k} = E_{k,loc} + P_k t_k \leq E_k. \quad (6)$$

In general, the circuit energy consumption is much lower than the communication and computation consumption, thus is neglected in this work. Similar to the existing works in [28], [31], the power consumption of IRS can be computed as $M\mu$, where μ indicates the power consumption of each passive element. Meanwhile, the IRS can only utilize the harvested energy to satisfy its circuit power consumption, thus the following constraint should be satisfied:

$$M\mu \left(\tau_2 + \sum_{k=1}^{K} t_k \right) \leq E_I. \quad (7)$$

III. COMPUTATION BITS MAXIMIZATION PROBLEM

In this section, we devote to maximize the total computation bits of all IoT devices, by jointly optimizing the uplink/downlink phase beamforming $\{\Gamma_d, \Gamma_{u,k}\}$ of the IRS, the time slot assignment $\{t_k\}$, the transmit power control $\{P_k\}$, and the CPU-cycle frequency of IoT devices $\{f_k\}$. The joint optimization problem will be

$$\begin{aligned} \underset{\Gamma_d, \Gamma_{u,k}, \tau_i, t_k, P_k, f_k}{\mathrm{maximize}} \quad & \sum_{k=1}^{K} Bt_k \log_2 \left(1 + \frac{P_k|\mathbf{g}_r^H \Gamma_{u,k} \mathbf{g}_{I,k} + g_{d,k}|^2}{\delta^2} \right) \\ & + \frac{f_k(T - t_0)}{C_k} \end{aligned}$$

$$\begin{aligned} \mathrm{s.t.} \quad & \mathrm{C1:} \; \kappa(T - t_0)f_k^3 + P_k t_k \leq \eta\tau_1 P_0 |h_{d,k}|^2 \\ & \quad + \eta\tau_2 P_0 |\mathbf{h}_{I,k}^H \Gamma_d \mathbf{h}_r + h_{d,k}|^2, \forall k \in \mathcal{K}, \\ & \mathrm{C2:} \; M\mu \left(\tau_2 + \sum_{k=1}^{K} t_k \right) \leq \eta\tau_1 P_0 \|\mathbf{h}_r\|^2, \\ & \mathrm{C3:} \; \sum_{i=0}^{K} t_i \leq T, \\ & \mathrm{C4:} \; \tau_1 + \tau_2 = t_0, \\ & \mathrm{C5:} \; 0 \leq \theta_{u.k.m} \leq 2\pi, \\ & \quad 0 \leq \theta_{d,m} \leq 2\pi, \forall k \in \mathcal{K}, \forall m \in \mathcal{M}, \\ & \mathrm{C6:} \; 0 \leq f_k \leq f_{k,\max}, \forall k \in \mathcal{K} \\ & \mathrm{C7:} \; 0 \leq P_0 \leq P_{0,\max}, \\ & \mathrm{C8:} \; 0 \leq t_k \leq T, \forall k \in \mathcal{K}. \end{aligned}$$

$$(8)$$

In (8), C1 and C2 indicate that the energy consumed by the k-th IoT device and the IRS should be less than their harvested downlink energy from the HAP, C3, C4 and C8 are the time constraints, C5 is the phase beamforming constraint, C6 represents the maximum CPU frequency constraints of IoT devices, and C7 restricts the maximum transmit power at the HAP.

Remark 1: Problem (8) is a non-convex non-linear optimization problem, which is challenging to obtain its global optimal solution in polynomial time, due to the highly coupled variables, e.g., the coupling between the transmit power P_k and the uplink phase beamforming matrix $\Gamma_{u,k}$, the coupling between P_k and t_k, as well as the coupling between t_0 and f_k.

To solve problem (8), the following result is first proposed as follows.

Theorem 1: In (8), the maximum computation bits are achieved when $P_0^* = P_{0,\max}$.

Proof: Obviously, a larger transmission power at the HAP implies that the IoT devices will harvest more radio-frequency energy from the HAP. Hence, the IoT device can improve its CPU frequency or uplink transmission power for processing more tasks through local computing or computation offloading. As a result, the maximum computation bits are achieved when the HAP adopts the maximum transmit power, namely $P_0^* = P_{0,\max}$. ∎

Then, the classic block coordinate descent method is exploited to convert the non-convex non-linear problem (8) into four subproblem, namely transmit power and time optimization, downlink energy beamforming optimization, uplink phase beamforming optimization, and local CPU-cycle frequency optimization subproblems. The corresponding flow chart is illustrated in Fig. 2.
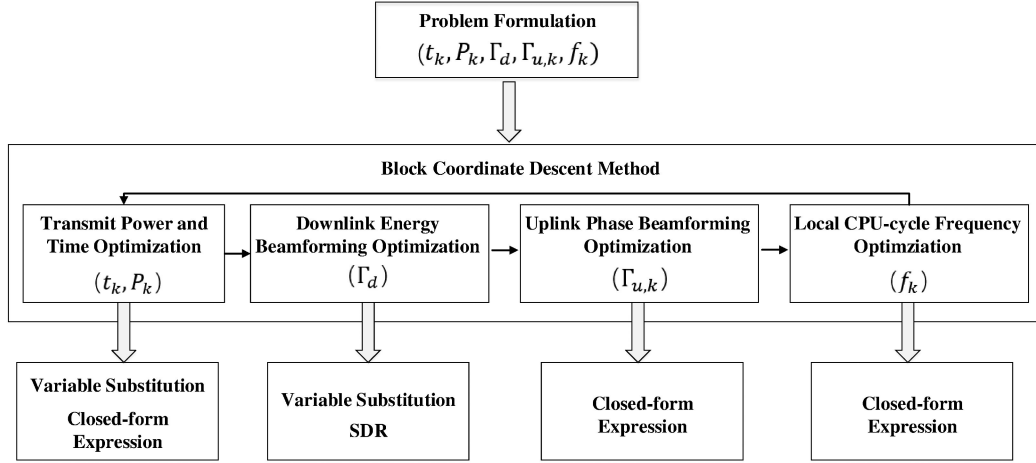
Fig. 2. The flow chart of the proposed alternative optimization method.

A. Transmit Power and Time Optimization

For given $\{\Gamma_d^*, \Gamma_{u,k}^*, f_k^*\}$ (8) will be converted to the transmit power and time slot allocation subproblem

$$\underset{\tau_i, t_k, P_k}{\text{maximize}} \sum_{k=1}^{K} Bt_k \log_2\left(1 + \frac{P_k|\mathbf{g}_r^H \Gamma_{u,k}^* \mathbf{g}_{I,k} + g_{d,k}|^2}{\delta^2}\right)$$

$$+ \frac{f_k^*(T - t_0)}{C_k}$$

$$\text{s.t.} \quad \kappa(T - t_0)(f_k^*)^3 + P_k t_k \leq \eta\tau_1 P_{0,\max}|h_{d,k}|^2$$

$$+ \eta\tau_2 P_{0,\max}|\mathbf{h}_{I,k}^H \Gamma_d^* \mathbf{h}_r + h_{d,k}|^2, \forall k \in \mathcal{K},$$

$$\text{C2–C4, C8.} \tag{9}$$

In order to tackle the coupled time and power variables, we introduce a set of energy variables, i.e., $e_k = t_k P_k$, to reformulate the problem (9) as

$$\underset{\tau_i, t_k, e_k}{\text{maximize}} \sum_{k=1}^{K} D_k(t_0, t_k, f_k^*, e_k, \Gamma_{u,k}^*) \tag{10a}$$

$$\text{s.t.} \quad \begin{aligned} E_{c,k}(t_0, f_k^*, e_k) &\leq \eta P_{0,\max}\tau_1|h_{d,k}|^2 \\ &+ \eta P_{0,\max}\tau_2|\mathbf{h}_{I,k}^H \Gamma_d^* \mathbf{h}_r + h_{d,k}|^2, \forall k \in \mathcal{K}, \end{aligned} \tag{10b}$$

$$M\mu\left(\tau_2 + \sum_{k=1}^{K} t_k\right) \leq \eta P_{0,\max}\tau_1\|\mathbf{h}_r\|^2, \tag{10c}$$

$$\text{C3-C4, C8.} \tag{10d}$$

where

$$D_k(t_0, t_k, f_k^*, e_k, \Gamma_{u,k}^*) =$$

$$Bt_k \log_2\left(1 + \frac{e_k|\mathbf{g}_r^H \Gamma_{u,k}^* \mathbf{g}_{I,k} + g_{d,k}|^2}{t_k\delta^2}\right) + \frac{f_k^*(T - t_0)}{C_k}, \tag{11}$$

$$E_{c,k}(t_0, f_k^*, e_k) = \kappa(T - t_0)(f_k^*)^3 + e_k. \tag{12}$$

Theorem 2: (10) is a convex optimization problem.

Proof: First, we need to prove that that the objective function (10a) is concave. Obviously, $B \log_2(1 + \frac{e_k|\mathbf{g}_r^H \Gamma_{u,k}^* \mathbf{g}_{I,k} + g_{d,k}|^2}{\delta^2})$ is a concave function of e_k, thus its perspective function $Bt_k \log_2(1 + \frac{e_k|\mathbf{g}_r^H \Gamma_{u,k}^* \mathbf{g}_{I,k} + g_{d,k}|^2}{t_k\delta^2})$ is also a concave function of t_k and e_k. Therefore, the objective function (10a) are concave. Since the other constraints are linear, thus we can derive that problem (10) is a convex optimization problem. ∎

Next, the optimal solution $\{\tau_i^*, t_k^*, e_k^*\}$ will be derived in closed-form expressions, in order to to gain more meaningful insights.

Theorem 3: The optimal τ_1^* is given by

$$\tau_1^* = \frac{M\mu T}{M\mu + \eta P_{0,\max}\|\mathbf{h}_r\|^2}. \tag{13}$$

Proof: As observed from problem (10), the total computation rate increases monotonously with t_k and e_k. Therefore, the constraint (10c) must be satisfied with equality in the optimal solution of (10). If $M\mu(\tau_2 + \sum_{k=1}^{K} t_k) < \eta P_{0,\max}\tau_1\|\mathbf{h}_r\|^2$, we can decrease τ_1 and increase τ_2 for increasing the harvested energy at the IoT devices, which will further result in a larger number of total accomplished computation tasks. Meanwhile, it is easy to understand that constraint C3 must be satisfied with equality. Combined C3-C4 and (10c), we have

$$M\mu\left(T - \tau_1^*\right) = \eta P_{0,\max}\tau_1^*\|\mathbf{h}_r\|^2. \tag{14}$$

After some simple calculations, we can derive the result presented in (13). ∎

Remark 2: It can be seen from (13) that the optimal τ_1^* is related to the number of reflection elements M, the power consumption for each reflection element μ, maximum transmission power of HAP, and the time block length T. Clearly, the IRS will harvest enough energy with a shorter duration, when the HAP adopts a higher downlink transmission power. In addition, with a longer time block length T or a higher power consumption μ for each reflection element or a larger number of reflection units M, the IRS must harvest more energy to keep its operation in the considered time block, which will further lead to a larger energy harvesting duration τ_1.

Theorem 4: The optimal e_k^* is derived as

$$e_k^* = a_k + b_k\tau_2^*, \tag{15}$$

where

$$a_k = \eta P_{0,\max}\tau_1^*|h_{d,k}|^2 - \kappa(T - \tau_1^*)(f_k^*)^3, \tag{16}$$

$$b_k = \eta P_{0,\max}|\mathbf{h}_{I,k}^H\Gamma_d^*\mathbf{h}_r + h_{d,k}|^2 + \kappa(f_k^*)^3. \tag{17}$$

Proof: Clearly, the maximum computation rate is achieved when the IoT devices use up all their harvested energy, i.e.,

$$\begin{aligned}
e_k^* &= \eta P_{0,\max}\tau_1|h_{d,k}|^2 + \eta P_{0,\max}\tau_2|\mathbf{h}_{I,k}^H\Gamma_d^*\mathbf{h}_r + h_{d,k}|^2 \\
&\quad - \kappa(T - \tau_1^* - \tau_2^*)(f_k^*)^3 \\
&= a_k + b_k\tau_2^*.
\end{aligned} \tag{18}$$

∎

Theorem 5: The optimal $\{\tau_2^*, t_k^*\}$ will be

$$\tau_2^* = \frac{T - \tau_1^* - \sum_{k=1}^K \frac{a_k}{x_k^*\delta^2}}{1 + \sum_{k=1}^K \frac{b_k}{x_k^*\delta^2}}, \tag{19}$$

$$t_k^* = \frac{a_k + b_k\tau_2^*}{x_k^*\delta^2}, \tag{20}$$

where x_k^* represents the unique solution of $\frac{B}{\log 2}(\frac{x_k^*}{1+x_k^*} - \log(1 + x_k^*)) - \sum_{k=1}^K(\frac{f_k^*}{C_k} - \frac{Bb_k/\delta^2}{\log 2(1+x_k^*)}) = 0$.

Proof: See Appendix A. ∎

B. Downlink Energy Beamforming Optimization

For given $\{t_k^*, P_k^*, f_k^*, \Gamma_{u,k}^*\}$, (8) reduces to the downlink energy beamforming optimization subproblem

$$\underset{\Gamma_d}{\text{Find}} \ \Gamma_d \tag{21a}$$

$$\text{s.t.} \quad \begin{aligned}
&E_{c,k}(t_0^*, f_k^*, P_k^*) \leq \eta\tau_1^*P_0^*|h_{d,k}|^2 \\
&+ \eta P_0^*\tau_2^*|\mathbf{h}_{I,k}^H\Gamma_d\mathbf{h}_r + h_{d,k}|^2, \forall k \in \mathcal{K},
\end{aligned} \tag{21b}$$

$$0 \leq \theta_{d,m} \leq 2\pi, \forall m \in \mathcal{M}, \tag{21c}$$

where $E_{c,k}(t_0^*, f_k^*, P_k^*) = \kappa(T - t_0^*)(f_k^*)^3 + P_k^*t_k^*$. We set $\mathbf{v}_d = (e^{j\theta_{d,1}}, \ldots, e^{j\theta_{d,M}})^T$, $\hat{\mathbf{v}}_d = [\mathbf{v}_d, 1]^T$, $\mathbf{h}_k^H = [\mathbf{h}_{I,k}^H\text{diag}(\mathbf{h}_r), h_{d,k}]$. Since $|\mathbf{h}_{I,k}^H\Gamma_d\mathbf{h}_r + h_{d,k}| = [\mathbf{h}_{I,k}^H\text{diag}(\mathbf{h}_r), h_{d,k}]\hat{\mathbf{v}}_d = \mathbf{h}_k^H\hat{\mathbf{v}}_d$, (21) will be rewritten as the following problem

$$\underset{\hat{\mathbf{v}}_d}{\text{Find}} \ \hat{\mathbf{v}}_d \tag{22a}$$

$$\text{s.t.} \quad \begin{aligned}
&E_{c,k}(t_0^*, f_k^*, P_k^*) \leq \eta\tau_1^*P_0^*|h_{d,k}|^2 \\
&+ \eta P_0^*\tau_2^*|\mathbf{h}_k^H\hat{\mathbf{v}}_d|^2, \forall k \in \mathcal{K},
\end{aligned} \tag{22b}$$

$$[\hat{\mathbf{v}}_d\hat{\mathbf{v}}_d^H]_{mm} = 1, \forall m \in \mathcal{M}. \tag{22c}$$

To address the non-linear equality constraint (22c), we introduce a matrix variable $\hat{\mathbf{V}}_d = \hat{\mathbf{v}}_d\hat{\mathbf{v}}_d^H$, and (22) will be converted to the following problem

$$\underset{\hat{\mathbf{v}}_d}{\text{Find}} \ \hat{\mathbf{V}}_d \tag{23a}$$

$$\text{s.t.} \quad \begin{aligned}
&E_{c,k}(t_0^*, f_k^*, P_k^*) \leq \eta\tau_1^*P_0^*|h_{d,k}|^2 \\
&+ \eta P_0^*\tau_2^*\text{Tr}(\mathbf{H}_k^H\hat{\mathbf{V}}_d), \forall k \in \mathcal{K}
\end{aligned} \tag{23b}$$

$$[\hat{\mathbf{V}}_d]_{mm} = 1, \forall m \in \mathcal{M}, \tag{23c}$$

$$\hat{\mathbf{V}}_d \succeq 0, \tag{23d}$$

$$\text{Rank}(\hat{\mathbf{V}}_d) = 1, \tag{23e}$$

where $\mathbf{H}_k = \mathbf{h}_k\mathbf{h}_k^H$. Due to the non-convex rank-one constraint (23e), we will adopt the SDR method to relax it. Obviously, the relaxed version of (23) is convex and can be solved via classic convex toolboxes, such as Yalmip and CVX. However, the optimal solution of (23) cannot be ensured rank-one, thus we will further adopt the Gaussian randomization method to recover the rank-one solution of (23) [47].

C. Uplink Phase Beamforming Optimization

Under given $\{t_k^*, P_k^*, f_k^*, \Gamma_d^*\}$, (8) reduces to the following uplink beamforming optimization subproblem

$$\underset{\Gamma_{u,k}}{\text{maximize}} \ \sum_{k=1}^K Bt_k^* \log_2\left(1 + \frac{P_k^*|\mathbf{g}_r^H\Gamma_{u,k}\mathbf{g}_{I,k} + g_{d,k}|^2}{\delta^2}\right) \tag{24a}$$

$$\text{s.t.} \quad 0 \leq \theta_{U.K.m} \leq 2\pi, \forall k \in \mathcal{K}, \forall m \in \mathcal{M}, \tag{24b}$$

We see that the task offloading rate of the k-th IoT device increases monotonically with $|\mathbf{g}_r^H\Gamma_{u,k}\mathbf{g}_{I,k} + g_{d,k}|^2$. Therefore, the optimal solution of (24) can be obtained by independently solving the following optimization problem during the k-th offloading time slot t_k, i.e.,

$$\underset{\Gamma_{u,k}}{\text{maximize}} \ |\mathbf{g}_r^H\Gamma_{u,k}\mathbf{g}_{I,k} + g_{d,k}|^2 \tag{25a}$$

$$\text{s.t.} \quad 0 \leq \theta_{U.K.m} \leq 2\pi, \forall k \in \mathcal{K}, \forall m \in \mathcal{M}, \tag{25b}$$

Theorem 6: The optimal IRS phase shifts for uplink task offloading can be derived as

$$\theta_{u,k,m}^* = \arg(g_{d,k}) - \arg(\mathbf{g}_k[m]) \tag{26}$$

Proof: Let us denote $\mathbf{v}_{u,k} = (e^{j\theta_{U.K.1}}, \ldots, e^{j\theta_{U.K.M}})^T$ and $\mathbf{g}_k = \text{diag}(\mathbf{g}_r^H)\mathbf{g}_{I,k}$, thus we have

$$|\mathbf{g}_r^H\Gamma_{u,k}\mathbf{g}_{I,k} + g_{d,k}|^2 = |\mathbf{v}_{u,k}^T\text{diag}(\mathbf{g}_r^H)\mathbf{g}_{I,k} + g_{d,k}|^2 \tag{27a}$$

$$= |\mathbf{v}_{u,k}^T\mathbf{g}_k + g_{d,k}|^2 \tag{27b}$$

$$\leq |\mathbf{v}_{u,k}^T\mathbf{g}_k|^2 + |g_{d,k}|^2 + 2|\mathbf{v}_{u,k}^T\mathbf{g}_k||g_{d,k}|. \tag{27c}$$

The equality of (27c) holds when $\arg(\mathbf{v}_{u,k}^T\mathbf{g}_k) = \arg(g_{d,k})$. Therefore, the optimal solution of (25) can be expressed as

$$\theta_{u,k,m}^* = \arg(\mathbf{v}_{u,k}[m]) = \arg(g_{d,k}) - \arg(\mathbf{g}_k[m]). \tag{28}$$

∎

Remark 3: According to Theorem 6, we find that the optimal phase beamforming matrix $\Gamma_{u,k}^*$ should be adjusted such that the uplink cascaded link $\mathbf{g}_r^H\Gamma_{u,k}^*\mathbf{g}_{I,k}$ via IRS aligns with its direct link $g_{d,k}$, namely $\mathbf{g}_r^H\Gamma_{u,k}^*\mathbf{g}_{I,k} = \beta_k g_{d,k}$, where β_k is constant. Therefore, the received signal to noise ratio at the HAP for

decoding the computation task offloaded by the k-th IoT device can be improved up to $1 + \beta_k^2$, when compared to the counterpart without IRS.

D. Local CPU-Cycle Frequency Optimization

Under given $\{t_k^*, P_k^*, \Gamma_d^*, \Gamma_{u,k}^*\}$, (8) reduces to the following local CPU-cycle frequency optimization subproblem

$$\underset{f_k}{\text{maximize}} \sum_{k=1}^{K} \frac{f_k(T - t_0^*)}{C_k} \tag{29a}$$

$$\text{s.t.} \quad \kappa(T - t_0^*)f_k^3 + P_k^* t_k^* \leq E_k(\tau_1^*, \tau_2^*, P_0^*, \Gamma_d^*), \forall k \in \mathcal{K}, \tag{29b}$$

$$0 \leq f_k \leq f_{k,\max}, \forall k \in \mathcal{K}, \tag{29c}$$

where

$$E_k(\tau_1^*, \tau_2^*, P_0^*, \Gamma_d^*) = \eta \tau_1^* P_0^* |h_{d,k}|^2$$
$$+ \eta P_0^* \tau_2^* |\mathbf{h}_{I,k}^H \Gamma_d^* \mathbf{h}_r + h_{d,k}|^2. \tag{30}$$

We observe that problem (29) is a linear programming problem. Then, we will derive the optimal CPU-cycle frequency in closed-form expression as follows.

Theorem 7: The optimal local CPU frequencies of (29) will be

$$f_k^* = \min\left\{ f_{k,\max}, \sqrt[3]{\frac{E_k(\tau_1^*, \tau_2^*, P_0^*, \Gamma_d^*) - P_k^* t_k^*}{\kappa(T - t_0^*)}} \right\} \tag{31}$$

Proof: According to the constraints in (29), we can derive that

$$0 \leq f_k \leq \min\left\{ f_{k,\max}, \sqrt[3]{\frac{E_k(\tau_1^*, \tau_2^*, P_0^*, \Gamma_d^*) - P_k^* t_k^*}{\kappa(T - t_0^*)}} \right\}. \tag{32}$$

The objective function (29a) increases monotonically with the local CPU-cycle frequency f_k. Therefore, the optimal local CPU-cycle f_k^* is obtained at the upper bound of f_k, which completes our proof. ∎

According to above descriptions, this paper proposes an iterative algorithm for solving the computation bits maximization problem (8). All the optimization variables in (8) can be segmented into four blocks ($\{t_k, p_k\}, \hat{\mathbf{V}}_d, \Gamma_{u,k}, f_k$). Since the optimal uplink beamforming matrix is irrelevant to other variables, thus we first obtain the optimal $\Gamma_{u,k}^*$ according to Theorem 6. Then, the transmit power and time optimization $\{t_k, p_k\}$, downlink energy beamforming optimization $\hat{\mathbf{V}}_d$, and the local CPU-cycle frequency optimization $\{f_k\}$ are alternately optimized by solving (10), (23) and (29), respectively, and meanwhile guaranteeing the other optimization variables fixed. The detailed procedure is summarized in Algorithm 1.

E. Computational Complexity Analysis

The computational complexity of Algorithm 1 mainly consists of two parts, i.e., the iteration number and the per-iteration computational complexity. Let L denote the iteration number of Algorithm 1. At each iteration, two convex problems (10) and (23)

Algorithm 1: Alternating Optimization Method for Solving (8).

1 **Initialize:** Set $(t_k^{(n)}, p_k^{(n)}, \hat{\mathbf{V}}_d^{(n)}, \Gamma_{u,k}^{(n)}, f_k^{(n)})$, and $n = 1$.
2 Calculate the optimal uplink beamforming matrix $\Gamma_{u,k}^*$ according to the Theorem 6;
3 **Repeat:**
4   Solve (10) to obtain the optimal transmission energy and time allocation strategy $(t_k^{(n)}, e_k^{(n)})$;
5   Obtain the optimal $\hat{\mathbf{V}}_d^{(n)}$ via solving the relaxed version of (23);
6   Compute the optimal CPU-cycle frequency $f_k^{(n)}$ by utilizing the Theorem 7;
7   Update the iteration facrot $n = n + 1$;
8 **Until** convergence.
9 The Gaussian randomization method is exploited to recover the optimal rank-one phase beamforming matrix Γ_d^* from the optimal $\hat{\mathbf{V}}_d^*$.
10 **Obtaining** optimal solution $(t_k^*, p_k^* = \frac{e_k^*}{t_k^*}, \hat{\mathbf{V}}_d^*, \Gamma_{u,k}^*, f_k^*)$.

---

need to be addressed. Specifically, the joint transmit power optimization problem (10) is with $2(K + 1)$ variables and $3(K + 1)$ constraints. Therefore, the worst-case computational complexity for solving (10) will be $\mathcal{O}(20(K + 1)^3 \sqrt{3(K + 1)} \log(1/\epsilon_1))$ [48], where ϵ_1 denotes the tolerance factor. Similarly, the complexity for solving downlink phase beamforming optimization (23) is $\mathcal{O}((M^2 + K + M + 1)M^4 \sqrt{K + M + 1} \log(1/\epsilon_2))$. Besides, the computational complexity for obtaining the optimal uplink phase beamforming matrix and local CPU-cycle frequencies is negligible as compared to that of (10) or (23), since we derive their closed-form expressions. Therefore, the computational complexity of Algorithm 1 can be expressed as $\mathcal{O}(L(20(K + 1)^3 \sqrt{3(K + 1)} \log(1/\epsilon_1) + (M^2 + K + M + 1)M^4 \sqrt{K + M + 1} \log(1/\epsilon_2)))$.

Theorem 8: Algorithm 1 improves the objective function of (8) in each iteration, thus it can converge to the optimal solution.

Proof: See Appendix B. ∎

IV. NUMERICAL RESULTS

This section provides the simulation results to evaluate the total computation bits achieved by our proposed resource allocation strategy for IRS-assisted wireless powered MEC networks. For comparison, we also present the following two baseline methods:

- *Partial offloading without IRS:* The WET and task offloading are conducted without the aid of IRS.
- *Full offloading only:* Each IoT device executes their computation tasks only depending on the task offloading.

In simulation, the number of IoT devices is $K = 2$, the HAP is located at the original point, IRS is located at (0,5), while the IoT devices are located at the coordinates [(1,5), (2,4)]. The communication links are modeled as $\text{CL} = C_0 d t^{-\alpha} \mathbf{x}$, where

TABLE I
SIMULATION PARAMETERS

Parameters	Values
Number of IoT devices, K	2
Number of reflection elements, M	50
Path loss factor, $\alpha_r/\alpha_{I,k}/\alpha_{d,k}$	3/3/3.5
Time block length, T	1s
System bandwidth, B	5MHz
Maximum CPU-cycle frequency of IoT devices, $f_{k,\max}$	$[1 \times 10^7, 1.5 \times 10^7]$ cycles/s
Computational complexity, C_k	500 cycles/bit
The capacitance coefficient, κ	10^{-28}
Energy conversion efficiency, η	0.8
Maximum transmission power of HAP, $P_{0,\max}$	100W
Noise power, δ^2	10^{-7}W
Power consumption of each reflection unit, μ	1mW

Fig. 4. Total computation rate versus energy conversion efficiency.

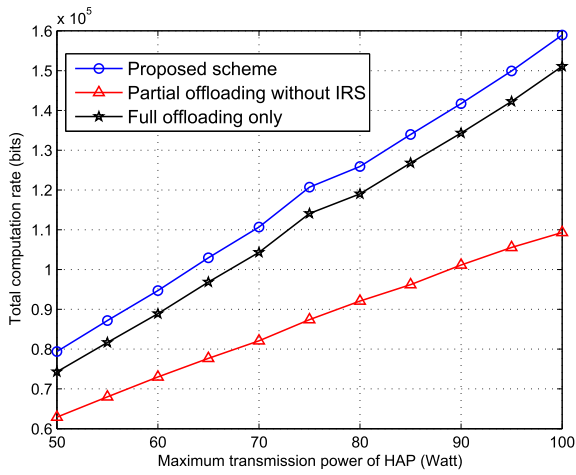Fig. 5. Total computation rate versus path loss factor $\alpha_{d,k}$.

Fig. 3. Total computation rate versus maximum transmission power of HAP.

$C_0 = -30$ dB represents the path loss at an unit distance, dt denotes the distance from the wireless transmitter to the corresponding receiver, α stands for the path loss factor of communication links, and $\mathbf{x}$ follows Rayleigh fading. Let α_r, $\alpha_{d,k}$ and $\alpha_{I,k}$ represent the path loss factor of the channel from from the HAP to the IRS, from the HAP to the k-th IoT device, and from the IRS to the k-th IoT device, respectively. The main simulation parameters are summarized in Table I. According to above parameter settings, the proposed algorithm is simulated by MATLAB R2012a.

In Fig. 3 and Fig. 4, we plot the total computation bits against the maximum transmission power of the HAP $P_{0,\max}$ and the energy conversion efficiency of IoT devices η, respectively. We see that the total computation rate for all the considered schemes increases monotonically with the increases of maximum transmission power of the HAP and the energy conversion efficiency. Obviously, the IoT devices will harvest more energy when the HAP adopts a higher transmission power or the energy harvesting circuit have a larger energy conversion efficiency, which will further result in that the IoT device can execute more
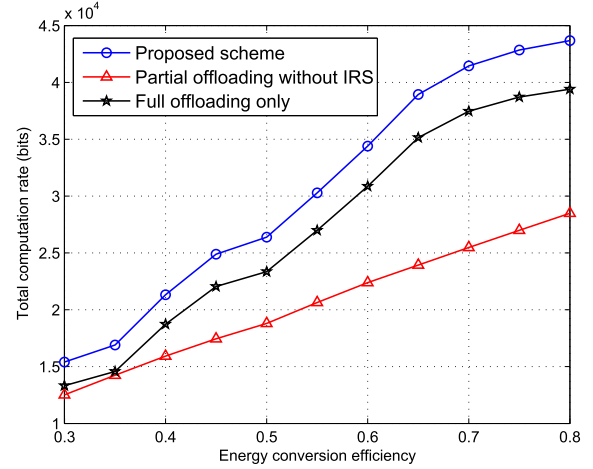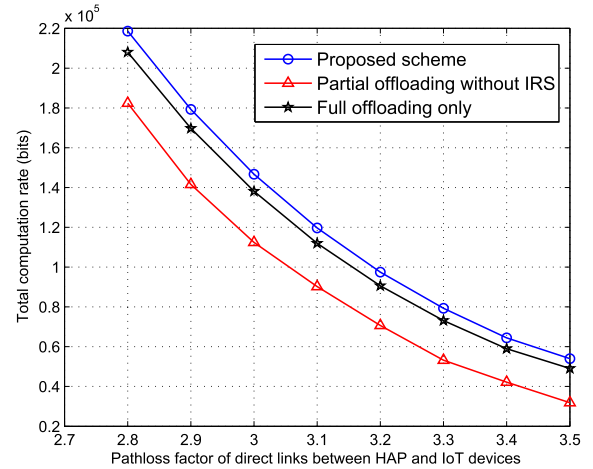
computation tasks via task offloading or local computing. Besides, we also see that the proposed strategy can achieve higher total computation rate as compared to the existing methods. In particular, the computation rate gain between the proposed method and the conventional method without the aid of IRS increases with the maximum transmission power of HAP and the energy conversion efficiency. It indicates that the reflecting link gain provided by the IRS can improve the task offloading rate significantly, when the IoT devices can harvest more energy with a larger $P_{0,\max}$ and η.

Fig. 5 shows the total computation rate versus the path loss factor of direct links between the HAP and IoT devices. As desired, we find that the total computation rate decreases with the increase of path loss factor. The reason is that a higher path loss factor $\alpha_{d,k}$ will result in a lower channel gain of the composite link between the HAP and the k-th IoT device. Moreover, our proposed IRS-assisted wireless powered MEC network can achieve 10% and 83% higher total computation rate than the full offloading scheme and the partial offloading scheme without the aid of IRS, respectively.

In Fig. 6, we plot the total computation rate against the task's computational complexity C_k. As can be observed, the total
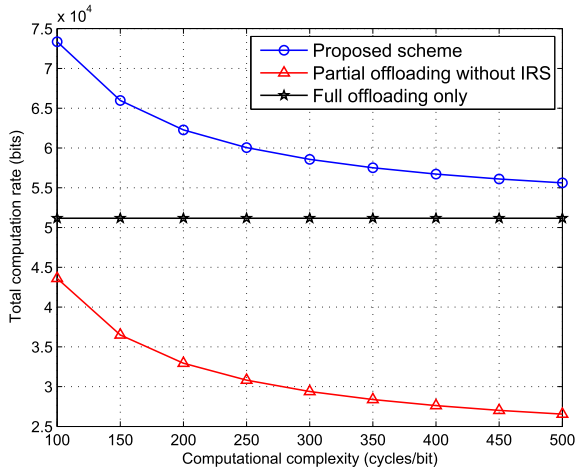
Fig. 6.   Total computation rate versus computational complexity.
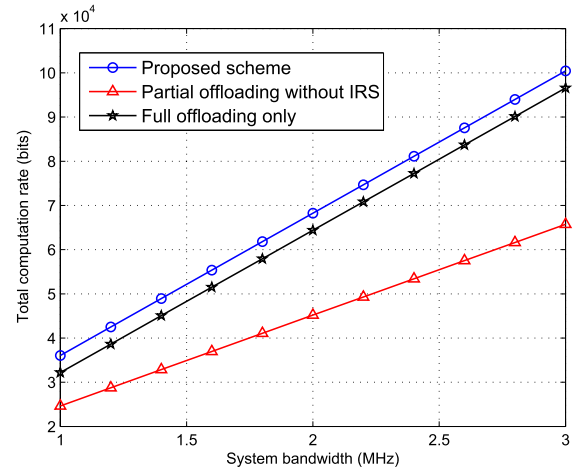

Fig. 8.   Total computation rate versus system bandwidth.
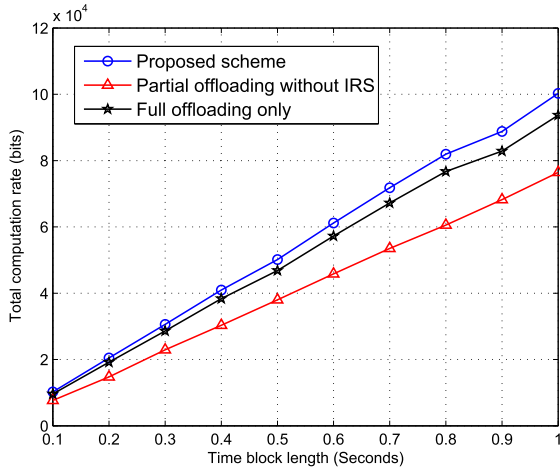

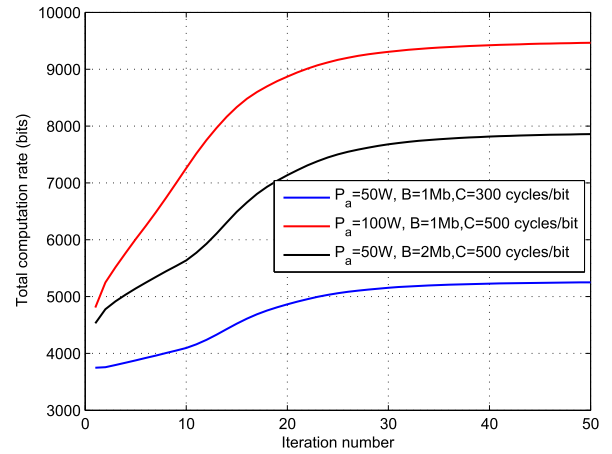Fig. 7.   Total computation rate versus time block length.

Fig. 9.   The convergence rate of Algorithm 1.

computation rate decreases with the increase of computational complexity for all these schemes. Besides, the rate gap between the proposed strategy and the full offloading strategy decreases along with the computational complexity C_k. This is mainly because that the computation offloading will be a more efficient way to execute the IoT devices' tasks than the local computing strategy, since the MEC server generally has more powerful computation capacity than IoT devices.

In Fig. 7 and Fig. 8, we reveal the total computation rate versus the time block length T and the system bandwidth B, respectively. We see that the total computation rate increases with the time block length and the system bandwidth. This is because that the computation offloading rate or the local computing rate increases with B and T. Moreover, we also observe that the proposed strategy can achieve higher computation rate gain than the baseline strategy without IRS, when the time block length is long. The reason is that a larger time block length will exert the full potential of IRS to improve the efficiency of WET and task offloading.

Fig. 9 plots the convergence curve of Algorithm 1 with different parameter settings. We see that the proposed algorithm will converge to the maximum computation rate less than thirty

iterations, which also implies that Algorithm 1 is computational efficient.

V. CONCLUSION

This paper studied the optimal resource management for IRS-enhanced wireless powered MEC networks. The downlink/uplink phase beamforming of IRS, local CPU frequencies of IoT devices, transmission power and time slot allocation for WET and task offloading were jointly scheduled to maximize the total computation bits under energy casuality constraints of IoT devices and IRS. To address the formulated non-convex non-linear optimization problem, we developed an iterative algorithm, and derived part of the optimal solutions in closed-form expressions. Finally, simulation results demonstrated that our proposed method can achieve higher total computation bits as compared to existing baseline methods.

Furthermore, our paper can be extended to several interesting future directions. First, non-orthogonal multiple access can be applied to improve the total computational rate. The key challenge in this scenario is how to utilize the IRS to suppress the co-channel interference introduced by the NOMA technique. In addition, multiple IRS can be properly deployed to further

improve the energy transfer efficiency and task offloading rate. However, it is essential to design low-complexity and robust phase beamforming optimization algorithm in the multi-IRS scenario.

APPENDIX A
PROOF OF THEOREM 5

By substituting the optimal $\{\tau_1^*, e_k^*\}$ into (10), we have

$$\max_{\tau_2, t_k} \sum_{k=1}^{K} Bt_k \log_2 \left(1 + \frac{a_k + b_k \tau_2}{t_k \delta^2}\right) + \frac{f_k^*(T - \tau_1^* - \tau_2)}{C_k} \quad (33\text{a})$$

$$\text{s.t.} \quad \tau_1^* + \tau_2 + \sum_{k=1}^{K} t_k \leq T, \quad (33\text{b})$$

$$\tau_2, t_k \geq 0, \forall k \in \mathcal{K}. \quad (33\text{c})$$

Then, we use the Karush-Kuhn-Tucker (KKT) condition to derive the optimal time assignment $\{\tau_2^*, t_k^*\}$ of problem (33). The Lagrange function of (33) will be

$$L(\tau_2, t_k, \lambda) = -\sum_{k=1}^{K} \left(Bt_k \log_2 \left(1 + \frac{a_k + b_k \tau_2}{t_k \delta^2}\right)\right.$$
$$+ \left.\frac{f_k^*(T - \tau_1^* - \tau_2)}{C_k}\right)$$
$$+ \lambda \left(\tau_1^* + \tau_2 + \sum_{k=1}^{K} t_k - T\right), \quad (34)$$

where λ denotes the dual variable related to the constraint (33b). The KKT conditions can be expressed as

$$\frac{\partial L}{\partial \tau_2} = \sum_{k=1}^{K} \left(\frac{f_k^*}{C_k} - \frac{Bb_k/\delta^2}{\log 2(1 + \frac{a_k + b_k \tau_2^*}{t_k^* \delta^2})}\right) + \lambda^* = 0, \quad (35)$$

$$\frac{\partial L}{\partial t_k} = \frac{B}{\log 2} \left(\frac{\frac{a_k + b_k \tau_2^*}{t_k \delta^2}}{1 + \frac{a_k + b_k \tau_2^*}{t_k \delta^2}} - \log \left(1 + \frac{a_k + b_k \tau_2^*}{t_k^* \delta^2}\right)\right)$$
$$+ \lambda^* = 0, \quad (36)$$

$$\lambda^* \left(\tau_1^* + \tau_2^* + \sum_{k=1}^{K} t_k^* - T\right) = 0, \quad (37)$$

where (35)–(36) represent the first-order derivative optimality conditions, (37) denotes the complementary slackness conditions. let us define $x_k^* = \frac{a_k + b_k \tau_2^*}{t_k^* \delta^2}$, the optimal x_k^* can be obtained by solving the following equations

$$F_k(x_k^*) = \frac{B}{\log 2} \left(\frac{x_k^*}{1 + x_k^*} - \log\left(1 + x_k^*\right)\right)$$
$$- \sum_{k=1}^{K} \left(\frac{f_k^*}{C_k} - \frac{Bb_k/\delta^2}{\log 2(1 + x_k^*)}\right) = 0, \quad (38)$$

where the first two terms of (38) is a monotonically increasing function with x_k^*, and the last term is with the same value for all IoT devices. Therefore, x_k^* is able to be obtained by using the

bisection method [49]. In addition, the maximum computation rate is achieved when the (33b) satisfies with equality, i.e.,

$$\tau_1^* + \tau_2^* + \sum_{k=1}^{K} t_k^* = \tau_1^* + \tau_2^* + \sum_{k=1}^{K} \frac{a_k + b_k \tau_2^*}{x_k^* \delta^2} = T. \quad (39)$$

After some simple transformations, the optimal time allocation will be derived as

$$\tau_2^* = \frac{T - \tau_1^* - \sum_{k=1}^{K} \frac{a_k}{x_k^* \delta^2}}{1 + \sum_{k=1}^{K} \frac{b_k}{x_k^* \delta^2}}, \quad (40)$$

$$t_k^* = \frac{a_k + b_k \tau_2^*}{x_k^* \delta^2}. \quad (41)$$

APPENDIX B
PROOF OF THEOREM 8

Denoting $D_k(t_k, e_k, \hat{\mathbf{V}}_d, \Gamma_{u,k}, f_k)$ as the objective function of the formulated computation bits maximization problem. According to the procedure of Algorithm, we can deduce that

$$D_k(t_k^{(n)}, e_k^{(n)}, \hat{\mathbf{V}}_d^{(n)}, \Gamma_{u,k}^*, f_k^{(n)}) \overset{(a1)}{\leq}$$
$$D_k(t_k^{(n+1)}, e_k^{(n+1)}, \hat{\mathbf{V}}_d^{(n)}, \Gamma_{u,k}^*, f_k^{(n)}) \overset{(a2)}{=}$$
$$D_k(t_k^{(n+1)}, e_k^{(n+1)}, \hat{\mathbf{V}}_d^{(n+1)}, \Gamma_{u,k}^*, f_k^{(n)}) \overset{(a3)}{\leq}$$
$$D_k(t_k^{(n+1)}, e_k^{(n+1)}, \hat{\mathbf{V}}_d^{(n+1)}, \Gamma_{u,k}^*, f_k^{(n+1)}) \quad (42)$$

where $a1$ holds because for given $(\hat{\mathbf{V}}_d^{(n)}, \Gamma_{u,k}^*, f_k^{(n)})$, $(t_k^{(n+1)}, e_k^{(n+1)})$ denotes the optimal solution to (10), a_2 holds since the objective function of the original problem (8) is not related to $\hat{\mathbf{V}}_d$, and a_3 holds because for given $(t_k^{(n+1)}, e_k^{(n+1)}, \hat{\mathbf{V}}_d^{(n+1)}, \Gamma_{u,k}^*)$, $f_k^{(n+1)}$ is the optimal solution to the local computing frequencies subproblem (29). Therefore, it proves that Algorithm 1 improves the objective function of (8) in each iteration. Integrated with the boundedness of maximum achievable computation bits, we can derive that the proposed Algorithm 1 is able to coverage to an optimal solution.

REFERENCES

[1] X. Wang, Y. Han, V. C. M. Leung, D. Niyato, X. Yan, and X. Chen, "Convergence of edge computing and deep learning: A comprehensive survey," *IEEE Commun. Surv. Tut.*, vol. 22, no. 2, pp. 869–904, Second Quarter 2020.

[2] Y. Chen, N. Zhang, Y. Zhang, X. Chen, W. Wu, and X. S. Shen, "Energy efficient dynamic offloading in mobile edge computing for Internet of Things," *IEEE Trans. Cloud Comput.*, vol. 9, no. 3, pp. 1050–1060, Jul.-Sep. 2021.

[3] X. Peng, K. Ota, and M. Dong, "Multiattribute-based double auction toward resource allocation in vehicular fog computing," *IEEE Internet Things J.*, vol. 7, no. 4, pp. 3094–3103, Apr. 2020.

[4] L. Liu *et al.*, "Blockchain-enabled secure data sharing scheme in mobile-edge computing: An asynchronous advantage actor-critic learning approach," *IEEE Internet Things J.*, vol. 8, no. 4, pp. 2342–2353, Feb. 2021.

[5] W. Huang, K. Ota, M. Dong, T. Wang, S. Zhang, and J. Zhang, "Result return aware offloading scheme in vehicular edge networks for IoT," *Comput. Commun.*, vol. 164, pp. 201–214, 2020.

[6] X. Chen, L. Jiao, W. Li, and X. Fu, "Efficient multi-user computation offloading for mobile-edge cloud computing," *IEEE/ACM Trans. Netw.*, vol. 24, no. 5, pp. 2795–2808, Oct. 2016.

[7] C. You, K. Huang, H. Chae, and B. Kim, "Energy-efficient resource allocation for mobile-edge computation offloading," *IEEE Trans. Wireless Commun.*, vol. 16, no. 3, pp. 1397–1411, Mar. 2017.

[8] Z. Chang, W. Guo, X. Guo, Z. Zhou, and T. Ristaniemi, "Incentive mechanism for edge-computing-based blockchain," *IEEE Trans. Ind. Inform.*, vol. 16, no. 11, pp. 7105–7114, Nov. 2020.

[9] J. Feng, F. R. Yu, Q. Pei, X. Chu, J. Du, and L. Zhu, "Cooperative computation offloading and resource allocation for blockchain-enabled mobile-edge computing: A deep reinforcement learning approach," *IEEE Internet Things J.*, vol. 7, no. 7, pp. 6214–6228, Jul. 2020.

[10] Z. Chang, L. Liu, X. Guo, and Q. Sheng, "Dynamic resource allocation and computation offloading for IoT fog computing system," *IEEE Trans. Ind. Informat.*, vol. 17, no. 5, pp. 3348–3357, May 2021.

[11] S. Gong *et al.*, "Toward smart wireless communications via intelligent reflecting surfaces: A contemporary survey," *IEEE Commun. Surv. Tut.*, vol. 22, no. 4, pp. 2283–2314, Fourth Quarter 2020.

[12] Q. Wu and R. Zhang, "Intelligent reflecting surface enhanced wireless network via joint active and passive beamforming," *IEEE Trans. Wireless Commun.*, vol. 18, no. 11, pp. 5394–5409, Nov. 2019.

[13] H. Yang, Z. Xiong, J. Zhao, D. Niyato, L. Xiao, and Q. Wu, "Deep reinforcement learning-based intelligent reflecting surface for secure wireless communications," *IEEE Trans. Wireless Commun.*, vol. 20, no. 1, pp. 375–388, Jan. 2021.

[14] C. Huang, A. Zappone, G. C. Alexandropoulos, M. Debbah, and C. Yuen, "Reconfigurable intelligent surfaces for energy efficiency in wireless communication," *IEEE Trans. Wireless Commun.*, vol. 18, no. 8, pp. 4157–4170, Aug. 2019.

[15] Q. Wu and R. Zhang, "Towards smart and reconfigurable environment: Intelligent reflecting surface aided wireless network," *IEEE Commun. Mag.*, vol. 58, no. 1, pp. 106–112, Jan. 2020.

[16] C. Huang *et al.*, "Holographic MIMO surfaces for 6G wireless networks: Opportunities, challenges, and trends," *IEEE Wireless Commun.*, vol. 27, no. 5, pp. 118–125, Oct. 2020.

[17] C. You, K. Huang, and H. Chae, "Energy efficient mobile cloud computing powered by wireless energy transfer," *IEEE J. Sel. Areas Commun.*, vol. 34, no. 5, pp. 1757–1771, May 2016.

[18] F. Wang, J. Xu, X. Wang, and S. Cui, "Joint offloading and computing optimization in wireless powered mobile-edge computing systems," *IEEE Trans. Wireless Commun.*, vol. 17, no. 3, pp. 1784–1797, Mar. 2018.

[19] S. Bi and Y. J. Zhang, "Computation rate maximization for wireless powered mobile-edge computing with binary computation offloading," *IEEE Trans. Wireless Commun.*, vol. 17, no. 6, pp. 4177–4190, Jun. 2018.

[20] S. Mao, S. Leng, S. Maharjan, and Y. Zhang, "Energy efficiency and delay tradeoff for wireless powered mobile-edge computing systems with multi-access schemes," *IEEE Trans. Wireless Commun.*, vol. 19, no. 3, pp. 1855–1867, Mar. 2020.

[21] X. Hu, K. Wong, and K. Yang, "Wireless powered cooperation-assisted mobile edge computing," *IEEE Trans. Wireless Commun.*, vol. 17, no. 4, pp. 2375–2388, Apr. 2018.

[22] S. Mao, J. Wu, L. Liu, D. Lan, and A. Taherkordi, "Energy-efficient cooperative communication and computation for wireless powered mobile-edge computing," *IEEE Syst. J.*, to be published, doi: 10.1109/JSYST.2020.3020474.

[23] F. Zhou, Y. Wu, R. Q. Hu, and Y. Qian, "Computation rate maximization in UAV-enabled wireless-powered mobile-edge computing systems," *IEEE J. Sel. Areas Commun.*, vol. 36, no. 9, pp. 1927–1941, Sep. 2018.

[24] F. Zhou and R. Q. Hu, "Computation efficiency maximization in wireless-powered mobile edge computing networks," *IEEE Trans. Wireless Commun.*, vol. 19, no. 5, pp. 3170–3184, May 2020.

[25] Q. Wu and R. Zhang, "Weighted sum power maximization for intelligent reflecting surface aided SWIPT," *IEEE Wireless Commun. Lett.*, vol. 9, no. 5, pp. 586–590, May 2020.

[26] Q. Wu and R. Zhang, "Joint active and passive beamforming optimization for intelligent reflecting surface assisted SWIPT under QoS constraints," *IEEE J. Sel. Areas Commun.*, vol. 38, no. 8, pp. 1735–1748, Aug. 2020.

[27] C. Pan *et al.*, "Intelligent reflecting surface aided MIMO broadcasting for simultaneous wireless information and power transfer," *IEEE J. Sel. Areas Commun.*, vol. 38, no. 8, pp. 1719–1734, Aug. 2020.

[28] B. Lyu, P. Ramezani, D. T. Hoang, S. Gong, Z. Yang, and A. Jamalipour, "Optimized energy and information relaying in self-sustainable IRS-empowered WPCN," *IEEE Trans. Commun.*, vol. 69, no. 1, pp. 619–633, Jan. 2021.

[29] Y. Zheng, S. Bi, Y. J. Zhang, Z. Quan, and H. Wang, "Intelligent reflecting surface enhanced user cooperation in wireless powered communication networks," *IEEE Wireless Commun. Lett.*, vol. 9, no. 6, pp. 901–905, Jun. 2020.

[30] S. Hu, Z. Wei, Y. Cai, C. Liu, D. W. K. Ng, and J. Yuan, "Robust and secure sum-rate maximization for multiuser MISO downlink systems with self-sustainable IRS," 2021, *arXiv:2101.10549*.

[31] Y. Zou, S. Gong, J. Xu, W. Cheng, D. T. Hoang, and D. Niyato, "Wireless powered intelligent reflecting surfaces for enhancing wireless communications," *IEEE Trans. Veh. Technol.*, vol. 69, no. 10, pp. 12 369–12 373, Oct. 2020.

[32] T. Bai, C. Pan, Y. Deng, M. Elkashlan, A. Nallanathan, and L. Hanzo, "Latency minimization for intelligent reflecting surface aided mobile edge computing," *IEEE J. Sel. Areas Commun.*, vol. 38, no. 11, pp. 2666–2682, Jul. 2020.

[33] F. Zhou, C. You, and R. Zhang, "Delay-optimal scheduling for IRS-aided mobile edge computing," *IEEE Wireless Commun. Lett.*, vol. 10, no. 4, pp. 740–744, Apr. 2021.

[34] S. Mao, X. Chu, Q. Wu, L. Liu, and J. Feng, "Intelligent reflecting surface enhanced D2D cooperative computing," *IEEE Wireless Commun. Lett.*, vol. 10, no. 7, pp. 1419–1423, Jul. 2021.

[35] Z. Chu, P. Xiao, M. Shojafar, D. Mi, J. Mao, and W. Hao, "Intelligent reflecting surface assisted mobile edge computing for Internet of Things," *IEEE Wireless Commun. Lett.*, vol. 10, no. 3, pp. 619–623, Mar. 2021.

[36] X. Hu, C. Masouros, and K.-K. Wong, "Reconfigurable intelligent surface aided mobile edge computing: From optimization-based to location-only learning-based solutions," *IEEE Trans. Commun.*, vol. 69, no. 6, pp. 3709–3725, Jun. 2021.

[37] Y. Liu *et al.*, "Intelligent reflecting surface meets mobile edge computing: Enhancing wireless communications for computation offloading," 2020, *arXiv:2001.07449*.

[38] T. Bai, C. Pan, H. Ren, Y. Deng, M. Elkashlan, and A. Nallanathan, "Resource allocation for intelligent reflecting surface aided wireless powered mobile edge computing in OFDM systems," *IEEE Trans. Wireless Commun.*, vol. 20, no. 8, pp. 5389–5407, Aug. 2021.

[39] Z. Chang, Z. Wang, X. Guo, C. Yang, Z. Han, and T. Ristaniemi, "Distributed resource allocation for energy efficiency in OFDMA multicell networks with wireless power transfer," *IEEE J. Sel. Areas Commun.*, vol. 37, no. 2, pp. 345–356, Feb. 2019.

[40] Q. Wu, M. Tao, D. W. Kwan Ng, W. Chen, and R. Schober, "Energy-efficient resource allocation for wireless powered communication networks," *IEEE Trans. Wireless Commun.*, vol. 15, no. 3, pp. 2312–2327, Mar. 2016.

[41] S. Mao, S. Leng, J. Hu, and K. Yang, "Energy-efficient transmission schemes for cooperative wireless powered cellular networks," *IEEE Trans. Green Commun. Netw.*, vol. 3, no. 2, pp. 494–504, Jun. 2019.

[42] L. Ji and S. Guo, "Energy-efficient cooperative resource allocation in wireless powered mobile edge computing," *IEEE Internet Things J.*, vol. 6, no. 3, pp. 4744–4754, Jun. 2019.

[43] L. Huang, S. Bi, and Y.-J. A. Zhang, "Deep reinforcement learning for online computation offloading in wireless powered mobile-edge computing networks," *IEEE Trans. Mobile Comput.*, vol. 19, no. 11, pp. 2581–2593, Nov. 2020.

[44] X. Hu, K. Wong, K. Yang, and Z. Zheng, "UAV-assisted relaying and edge computing: Scheduling and trajectory optimization," *IEEE Trans. Wireless Commun.*, vol. 18, no. 10, pp. 4738–4752, Oct. 2019.

[45] X. Hu, K. K. Wong, and Y. Zhang, "Wireless-powered edge computing with cooperative UAV: Task, time scheduling and trajectory design," *IEEE Trans. Wireless Commun.*, vol. 19, no. 12, pp. 8083–8098, Dec. 2020.

[46] Y. Chen, N. Zhang, Y. Zhang, X. Chen, W. Wu, and X. S. Shen, "TOFFEE: Task offloading and frequency scaling for energy efficiency of mobile devices in mobile edge computing," *IEEE Trans. Cloud Comput.*, to be published, doi: 10.1109/TCC.2019.2923692.

[47] A. M.-C. So, J. Zhang, and Y. Ye, "On approximating complex quadratic optimization problems via semidefinite programming relaxations," *Math. Program.*, vol. 110, no. 1, pp. 93–110, 2007.

[48] Y. Dai, D. Xu, S. Maharjan, and Y. Zhang, "Joint computation offloading and user association in multi-task mobile edge computing," *IEEE Trans. Veh. Technol.*, vol. 67, no. 12, pp. 12 313–12 325, Dec. 2018.

[49] Q. Wu, W. Chen, D. W. K. Ng, and R. Schober, "Spectral and energy-efficient wireless powered iot networks: NOMA or TDMA?," *IEEE Trans. Veh. Technol.*, vol. 67, no. 7, pp. 6663–6667, Jul. 2018.

Sun Mao received the Ph.D. degree in communication and information systems from the University of Electronic Science and Technology of China, Chengdu, China, in 2020. From 2018 to 2019, he was with the University of Oslo, Oslo, Norway, as a visiting Ph.D. Student. He has authored or coauthored more than 20 papers at international journals and conferences, including IEEE TWC, IEEE TVT, IEEE TGCN, IEEE Systems Journal, IEEE WCL, IWQoS, ICC, Globecom, and WCNC. His research interests include simultaneous wireless information and power transfer, mobile edge computing, UAV communications, and intelligent reflecting surface-assisted wireless networks. He was the recipient of the best paper awards from IEEE Systems Journal-2021 and IEEE GreenCom-2017.

Ning Zhang (Senior Member, IEEE) received the Ph.D. degree from the University of Waterloo, Waterloo, ON, Canada, in 2015. He was a Postdoctoral Research Fellow with the University of Waterloo and also with the University of Toronto, Toronto, ON, Canada. He is currently an Associate Professor with the University of Windsor, Windsor, ON, Canada. He was the recipient of the best paper awards from IEEE Globecom in 2014, IEEE WCSP in 2015, and the *Journal of Communications and Information Networks* in 2018, IEEE ICC in 2019, the IEEE Technical Committee on Transmission Access and Optical Systems in 2019, and IEEE ICCC in 2019, respectively. He also serves/served as a Track Chair of several international conferences and the Co-Chair of several international workshops. He is an Associate Editor for the IEEE Internet of Things Journal, IEEE Transactions on Cognitive Communications and Networking, IEEE Access, *IET Communications*, and *Vehicular Communications*. He was a Guest Editor of several international journals, such as the IEEE Wireless Communications, IEEE Transactions on Industrial Informatics, and IEEE Transactions on Cognitive Communications and Networking.

Lei Liu (Member, IEEE) received the Ph.D. degree in telecommunications engineering from Xidian University, Xi'an, China, in 2019. He is currently a Lecture of telecommunications engineering with Xidian University. He has authored or coauthored more than 20 papers at international journals and conferences, which include IEEE TITS, IEEE IoTJ, IEEE TVT, ICC, PIMRC, and WPMC. His research interests include vehicular ad hoc networks, intelligent transportation, mobile edge computing, and Internet of Thing.

Jinsong Wu (Senior Member, IEEE) received the Ph.D. degree from the Department of Electrical and Computer Engineering, Queen's University, Kingston, ON, Canada. He was the Leading Editor and coauthor of the comprehensive book, entitled "*Green Communications: Theoretical Fundamentals, Algorithms, and Applications*," published by CRC Press in September 2012. He is elected the Vice-Chair, Technical Activities, IEEE Environmental Engineering Initiative, a pan-IEEE effort under IEEE Technical Activities Board (TAB). He was the Founder and Founding Chair of the IEEE Technical Committee on Green Communications and Computing (TCGCC). He is also the Co-Founder and Founding Vice-Chair of the IEEE Technical Committee on Big Data (TCBD). He was the recipient of the both 2017 and 2019 IEEE System Journal best paper awards. His co-authored paper won 2018 IEEE TCGCC Best Magazine Paper Award. He was the recipient of the IEEE Green Communications and Computing Technical Committee 2017 Excellent Services Award for Excellent Technical Leadership and Services in the Green Communications and Computing Community.

Mianxiong Dong (Member, IEEE) received the B.S., M.S., and Ph.D. degrees in computer science and engineering from the University of Aizu, Aizuwakamatsu, Japan. He became the youngest ever Professor with the Muroran Institute of Technology, Muroran, Japan, where he is currently serves as the Vice President. He was a JSPS Research Fellow with the School of Computer Science and Engineering, The University of Aizu, and was a Visiting Scholar with BBCR Group, University of Waterloo, Waterloo, ON, Canada, supported by JSPS Excellent Young Researcher Overseas Visit Program from April 2010 to August 2011. He was the recipient of the IEEE TCSC Early Career Award 2016, the IEEE SCSTC Outstanding Young Researcher Award 2017, the 12th IEEE ComSoc Asia-Pacific Young Researcher Award 2017, the Funai Research Award 2018, and the NISTEP Researcher 2018 (one of only 11 people in Japan) in recognition of significant contributions in science and technology. He is serving as the Vice Chair of IEEE Communications Society Asia/Pacific Region Information Services Committee and Meetings and Conference Committee, a Leading Symposium Chair of IEEE ICC 2019, a Student Travel Grants Chair of IEEE GLOBECOM 2019, and a Symposium Chair of IEEE GLOBECOM in 2016 and 2017. He is currently a Member of Board of Governors and the Chair of Student Fellowship Committee of IEEE Vehicular Technology Society, and a Treasurer of IEEE ComSoc Japan Joint Sections Chapter. He is Clarivate Analytics 2019 Highly Cited Researcher (Web of Science).

Kaoru Ota (Member, IEEE) received the B.S. degree in computer science and engineering from the University of Aizu, Aizuwakamatsu, Japan, in 2006, the M.S. degree in computer science from Oklahoma State University, Stillwater, OK, USA, in 2008, and the Ph.D. degree in computer science and engineering from the University of Aizu, in 2012. She is currently an Associate Professor with the Department of Sciences and Informatics, Muroran Institute of Technology, Muroran, Japan. From March 2010 to March 2011, she was a Visiting Scholar with University of Waterloo, Waterloo, ON, Canada. She is the Editor of the IEEE Transactions on Vehicular Technology (TVT), IEEE Internet of Things Journal, IEEE Communications Letters, *Peer-to-Peer Networking and Applications (Springer)*, *Ad Hoc and Sensor Wireless Networks*, *International Journal of Embedded Systems (Inderscience)*, and *Smart Technologies for Emergency Response and Disaster Management (IGI Global)*, and a Guest Editor of the *ACM Transactions on Multimedia Computing, Communications and Applications* (leading), IEEE Internet of Things Journal, IEEE Communications Magazine, IEEE Network, IEEE Wireless Communications, IEEE Access, *IEICE Transactions on Information and Systems*, and *Ad Hoc and Sensor Wireless Networks (Old City Publishing)*.

Tang Liu received the B.S. degree in computer science from the University of Electronic Science and Technology of China, Chengdu, China, in 2003, and the MS and Ph.D. degrees in computer science from Sichuan University, Chengdu, China, in 2009 and 2015, respectively. Since 2003, he has been with the College of Computer Science, Sichuan Normal University, Chengdu, China, where he is currently a Professor. From 2015 to 2016, he was a Visiting Scholar with the University of Louisiana at Lafayette, LA, USA. His research interests include wireless charging and wireless sensor networks.

Die Wu received the B.S. degree in information security and the Ph.D. degree in computer architecture from the Electronic Science and Technology of China, in 2011 and 2018, respectively. He is currently a Lecturer with the College of Computer Science, Sichuan Normal University, Chengdu, China. His research interests include RFID systems, wireless networks, and pervasive computing.